Journal of The Electrochemical Society, **158** (10) H1017-H1020 (2011)
0013-4651/2011/158(10)/H1017/4/$28.00 © The Electrochemical Society

Photovoltaic Performance of HWCVD Deposited μc-Si:H Solar Cells Using Graded Hydrogen Dilution Window-Layer

Uio-Pu Chiou,[a] Jia-Min Shieh,[b,c,z] Fu-Ming Pan,[a,z] and Wen-Hsien Huang[a,b]

[a]*Department of Materials and Engineering, National Chiao-Tung University, 1001 Ta-Hsueh Road, Hsinchu, 30010 Taiwan*
[b]*National Nano Device Laboratories, No. 26, Prosperity Road 1, Hsinchu 30078, Taiwan*
[c]*Department of Photonics and Institute of Electro-Optical Engineering, National Chiao-Tung University, Hsinchu 30010, Taiwan*

The study prepared thin film solar cells using hydrogenated microcrystalline silicon (μc-Si:H) by hot-wire chemical vapor deposition (HWCVD). Hydrogen dilution profiling was used to deposit the boron-doped p-layer on the SnO_2:F substrate. The μc-Si:H solar cell with triple hydrogen dilution grades in the p-layer has a high photoconversion efficiency of 4.5% as a result of the improvement in the electrical and the antireflection properties of the cell. The short circuit current (J_{sc}) and the open circuit voltage (V_{oc}) of the solar cell are 19.7 mA/cm^2 and 450 mV, respectively. The graded hydrogen concentration in the p-layer improves the crystallinity and the antireflection of the absorbing layer (intrinsic layer), thereby enhancing the J_{sc}. The high V_{oc} is ascribed to that a high hydrogen dilution ratio may enhance boron doping in the p-layer leading to the improvement of the V_{oc}.
© 2011 The Electrochemical Society. [DOI: 10.1149/1.3622290] All rights reserved.

Manuscript submitted April 20, 2011; revised manuscript received July 6, 2011. Published August 3, 2011.

The hydrogenated microcrystalline silicon (μc-Si:H) is considered a better photovoltaic material for thin film solar cell applications than amorphous silicon (a-Si:H) because of its stability against light degradation and excellent long wavelength response.[1] The conventional deposition techniques for thin film solar cells, such as plasma enhanced chemical vapor deposition (PECVD) and very-high frequency glow discharge (VHF-GD), can offer a high μc-Si:H deposition rate.[2] However, the plasma-assisted deposition may deteriorate the material and electrical properties of μc-Si:H thin films as a result of the plasma damage, and thus limits the development of μc-Si:H thin films and tandem solar cells.[3] Because hot-wire chemical vapor deposition (HWCVD) uses hot filament to catalytically decompose gas precursors. HWCVD is a plasma free deposition technique and can produce μc-Si:H thin films of lower defect density, lower hydrogen composition and smaller strain compared with plasma-assisted deposition methods.[4–6] It has been recently demonstrated that the cell performance of a single stacked p-i-n structure with μc-Si:H layers fabricated by HWCVD can be optimized by properly tuning deposition parameters to control the transition region between the μc-Si:H and the a-Si:H phase, which is usually formed in μc-Si:H thin films when plasma assisted CVD is performed.[7] The formation of the a-Si:H incubation layer will result in poor electron transport and a large amount of defects at the p/intrinsic layer (i-layer) interface due to heterogeneous growth,[8] therefore, retarding the growth of the incubation layer can improve the cell performance. It has been proposed that eliminating the incubation layer can also improve the crystallinity of the intrinsic μc-Si:H layer, thereby enhancing the electron-hole pair collection of the cell. This can be achieved by μc-Si:H deposition using hydrogen dilution profiling[9,10] or reverse hydrogen profiling.[4] Recently, a hydrogenated nanocrystalline silicon (nc-Si:H) structure consisting of a lightly hydrogen-diluted i/p buffer layer and a highly hydrogen-diluted p-layer was also demonstrated to reduce defects at the i/p interface and thus improve the a-Si:H n-i-p solar cell performance.[11] A buffer layer between the p-layer and the substrate can also improve the crystallinity of intrinsic layer and the optical absorption loss in the p-layer.[12] In this study, we prepared a novel "graded p-type window layer (GPL)" structure to exploit the dependence of the cell performance on the hydrogen concentration in the multilayer p-type window layer deposited by HWCVD. The a-Si:H incubation layer is absent in the HWCVD prepared GPL structure, and the crystallinity of the intrinsic layer is greatly improved. Moreover, the GPL structure also leads to a nearly omni-directional antireflection. The GPL-structured solar cell prepared by HWCVD has a conversion efficiency of 4.5% near the infrared wavelength regime.

[z] E-mail: fmpan@faculty.nctu.edu.tw; jmshieh@ndl.narl.org.tw

Experimental

The tungsten wire used as the catalytic filament has a diameter of 0.5 mm, a length of 10 cm, and the distance between the filament and the substrate was 5 cm. The filament and substrate temperature were controlled at 1800 and 200°C, respectively. The process pressure was 5–75 mtorr. The precursor gas mixture was composed of SiH_4 and H_2; PH_3 and B_2H_6 were used as the dopant gases. Figure 1a schematically shows the structure of the μc-Si:H thin-film solar cell with the GPL p-layer. The solar cells prepared by HWCVD comprises the Asahi U-type SnO_2:F substrate, the 30 nm thick p-layer, the 400 nm thick intrinsic layer, the 20 nm thick n-layer, the 80 nm thick ITO layer and the 1000 nm thick Al. The ITO/Al back reflector was prepared by DC-sputtering and defined the cell area of 0.09 cm^2. The GPL layer was deposited by tuning the hydrogen dilution ratio [$D_H = H_2/(SiH_4+H_2)$] during the HWCVD process using the gas mixture of SiH_4, H_2 and B_2H_6. Three GPL structures with different combinations of D_H in the p-layer were prepared: the singly graded p-layer (single-GPL), the doubly graded p-layer (double-GPL) and the triply graded p-layer (triple-GPL), which has the D_H combination of 93%, 93%/95% and 93%/95%/97%, respectively. During the deposition of the GPL layer, the hydrogen flow rate was changed stepwise in the order of increasing the D_H, and different hydrogen-diluted regions in a GPL multilayer were deposited with the same deposition time. Each of the three hydrogen-diluted regions in the 30 nm thick triple-GPL layer has a thickness of 10 nm. The D_H used for the deposition of the intrinsic layer and the n-layer was 92.8% and 92.3%, respectively. The microstructure of the solar cell structure was examined by high resolution transmission electron microscopy (HRTEM, JEM-2010F). Figure 1b shows a cross-sectional transmission electron micrograph of the solar cell with the triple-GPL layer. An x-ray diffractometer (XRD, PANalytical X'Pert Pro) with the Cu radiation (1.5418 Å) was used to study the crystallinity of the μc-Si:H thin-films. Absorption spectra were measured by Shimadzu UV-3101 PC spectrometer (300–900 nm). The current density–voltage (J-V) characteristics and the external quantum efficiency (QE) were measured under AM1.5 illumination.

Results and Discussion

Figure 2 shows XRD spectra of three different GPL structures without and with the intrinsic Si capping layer. The thickness of the intrinsic capping layer was only 50 nm instead of 400 nm so that we could properly examine the crystallinity of the intrinsic μc-Si:H deposited near the interface with the GPL structures. There are three barely discernible peaks in the spectra of the GPL samples before the deposition of the intrinsic layer (Fig. 2a). They are situated at 28.4, 47.2, and 56°, and correspond to the (111), (220) and (311)

Downloaded on 2014-04-24 to IP 140.113.38.11 address. Redistribution subject to ECS terms of use (see ecsdl.org/site/terms_use) unless CC License in place (see abstract).

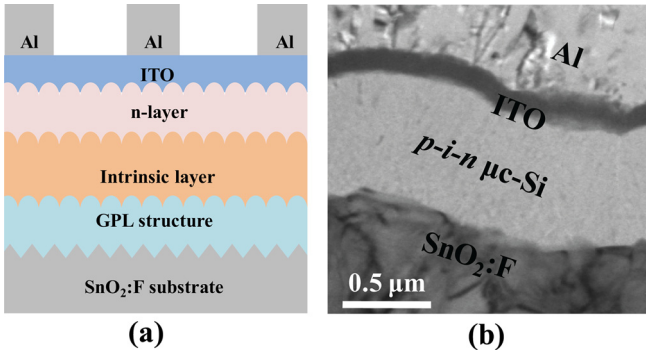

Figure 1. (Color online) (a) The schematic diagram of the μc-Si:H solar cell with the GPL-structured p-layer; the thickness of the p-layer is fixed at 30 nm for various GPL structures. (b) A cross-sectional TEM image of a triple-GPL structured solar cell.

lattice planes of the Si crystal, respectively. The very weak peak intensities of the boron-doped GPL layer may result from the small sampling thickness but is not due to a poor crystallinity because electron diffraction discussed below show clear diffraction rings. After the deposition of the intrinsic layer, the three diffraction peaks exhibit an obvious increase in the peak intensity. The intensity increase is particularly dramatic for the triple-GPL structure, indicating that the intrinsic layer on the triple-GPL structure has a much better crystallinity than that on the single-GPL and on the double-GPL structures. The better crystallinity of the intrinsic layer on the triple-GPL structure likely results from the higher D_H value in the topmost B-doped region, on which the intrinsic layer is directly grown. S.A. Filonovich *et al*. reported that a higher hydrogen dilution ratio could produce a μc-Si:H structure of better crystallinity in the p-layer.[13] Therefore, the well crystallized topmost region of the triple-GPL structure may facilitate the growth of an intrinsic layer of better crystallinity.

The HRTEM image of the μc-Si:H intrinsic layer deposited on the triple-GPL structure is shown in Fig. 3a. It can be clearly seen that, in the triple-GPL layer, μc-Si:H grains are embedded in the a-Si:H matrix near the SnO_2:F/triple-GPL interface. The selected area electron diffraction (SAD) pattern shown in Fig. 3b demonstrates the diffraction rings of the (111), (220) and (311) lattice planes. The a-Si:H incubation layer, which is usually observed in the p-layer deposited by PECVD, is absent at the interface between the GPL layer and the substrate. For the single- and the double-GPL structures, the a-Si:H incubation layer is not observed either in the TEM images (not shown). The TEM analysis suggests that the hydrogen dilution profiling deposition by HWCVD with a stepwise increased D_H can produce a p-layer of better crystallinity in comparison with plasma-assisted depositions. The plasma-damage free HWCVD seems to facilitate the phase transition from an amorphous-like polymorphous Si (pm-Si:H) state to the μc-Si:H phase during the early stage of the p-layer deposition, thereby retarding the amorphous incubation layer.[14–16] The absence of the amorphous incubation layer benefits crystal nucleation and growth on the substrate and thus results in good crystallinity in the p-layer.[16] Figure 3c shows a magnified image of a selected area (marked by the circle) of the intrinsic layer, and the corresponding SAD pattern of the area is shown in Fig. 3d. The lattice fringe labeled by the lines and arrows demonstrates the presence of μc-Si:H grains. The diffraction rings featuring distinct diffraction spots suggest that the intrinsic layer has a good crystallinity, and the (111), (220) and (311) lattice planes are the preferred orientation. This is in agreement with the XRD spectra shown in Fig. 2. The microstructure analyses indicate that the triple-GPL

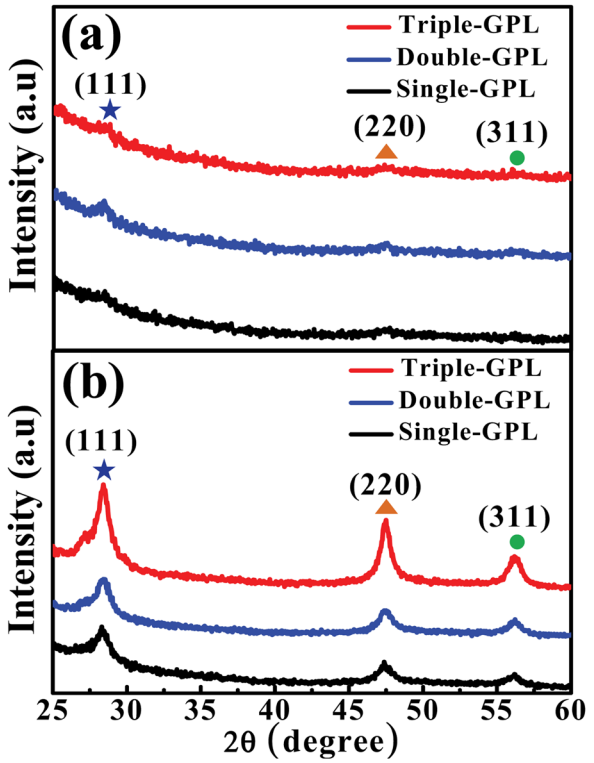

Figure 2. (Color online) XRD spectra of the 30 nm thick GPL-structured p-layer without (a) and with (b) a capping intrinsic layer with a thickness of 50 nm.

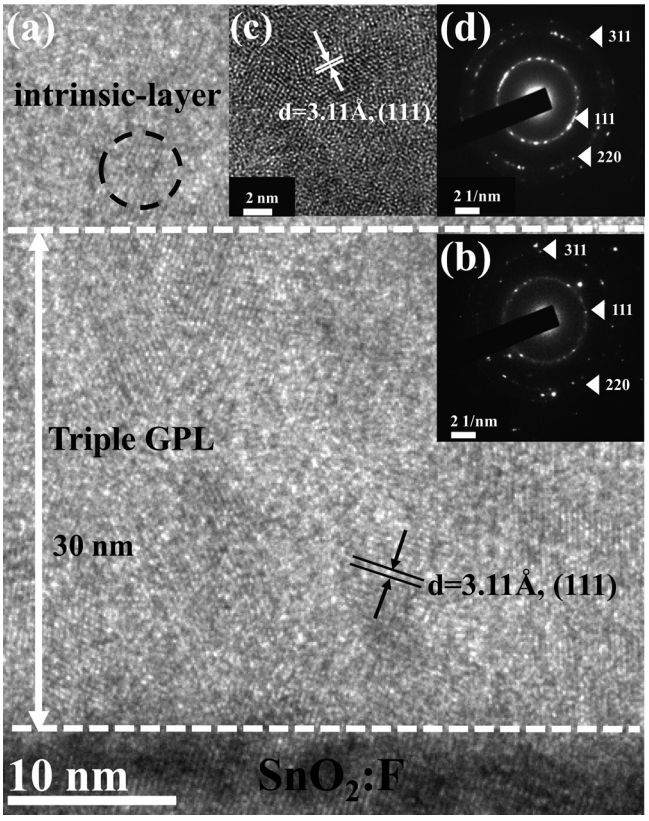

Figure 3. HRTEM images of (a) the triple-GPL structure as deposited on the SnO_2:F coated glass substrate, (b) the SAD images for the triple-GPL structure, (c) a magnified image of a selected area of the intrinsic layer shown in (a) and (d) SAD image of the intrinsic layer. The arrows mark the lattice orientation of the diffraction rings.

Downloaded on 2014-04-24 to IP 140.113.38.11 address. Redistribution subject to ECS terms of use (see ecsdl.org/site/terms_use) unless CC License in place (see abstract).

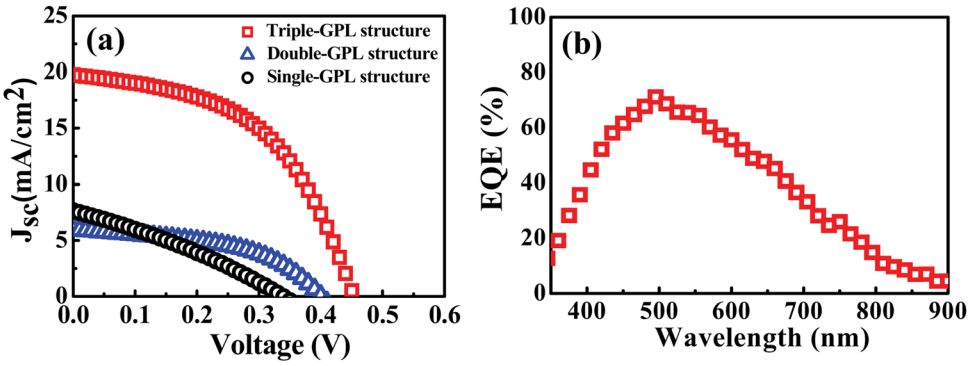

Figure 4. (Color online) (a)The J-V characteristics of the single-, double- and triple-GPL structured solar cells and (b) the external quantum efficiency of μc-Si:H triple-GPL structured solar cells.

structure can significantly improve the crystallinity of the intrinsic layer.

Figures 4a and 4b shows the J-V characteristics and external QE, respectively, of μc-Si:H solar cells with the three GPL structures. Table I lists values of the open circuit voltage (V_{oc}), the short circuit current (J_{sc}), the filling factor (FF) and the conversion efficiency (η) for the three solar cells. According to the table, the triple-GPL structured solar cell demonstrates the best photovotaic characteristics. This is likely due to the improved crystallinity and a higher hydrogen concentration in the intrinsic layer of the triple-GPL solar cell. The higher conversion efficiency (4.5%) of the triple-GPL solar cell is a result of the enhancement in the J_{sc} (19.7 mA/cm^2) and the V_{oc} (450 mV). The larger V_{oc} may be ascribed to a higher boron atomic concentration in the μc-Si:H p-layer. The V_{oc} of photovoltaic devices is determined by the saturated current, which is a function of the dopant concentration, as described by the following equations[17]:

$$V_{oc} = \frac{KT}{q}\ln\left(\frac{I_L}{I_0}\right) + 1 \quad [1]$$

$$I_0 = A\left(\frac{qD_e n_i^2}{L_e N_A} + \frac{qD_h n_i^2}{L_h N_D}\right) \quad [2]$$

where I_L is the light-generated current, I_0 the diode saturation current, K the Boltzmann's constant and T the temperature in degree Kelvin, n_i the intrinsic concentration, N_A the density of ionized acceptors, N_D the density of ionized donors, L_e the diffusion length of electron, L_h the diffusion length of hole; D_e and D_h are the diffusion constants of electron and holes, respectively. Because a high hydrogen atomic concentration can enhance boron diffusion in μc-Si:H thin films,[18] a GPL structure prepared with a larger D_H must have a higher boron concentration. According to eqs. 1 and 2, the increase of the dopant concentration will decrease I_0, and hence increase the V_{oc}. Therefore, the V_{oc} of the three solar cells increases in the sequence of single-GPL< double-GPL< triple-GPL structures.

The QE curve of the μc-Si:H thin film solar cell with the triple-GPL structure is given in Fig. 4b. The triple-GPL structured solar cell has a high QE response in the wavelength range between 650 and 800 nm. The high QE in the near infrared range can be ascribed to the high absorption in the optical range, which enhances light absorption leading to a higher electron-hole pair generation, thereby increasing the J_{sc}. Figure 5 shows absorption spectra of the single-, double- and triple-GPL structures capping a 50 nm thick intrinsic layer. The triple-GPL structure has a much higher photon absorption in the near infrared (IR) regime than the other two GPL structures. The additional absorption in the IR range is likely a result of the improved crystallinity of the μc-Si:H phase in the intrinsic layer. Compared with a-Si:H, μc-Si:H has a smaller band gap and can absorb photons of longer wavelength (near infrared range).[1,19] Therefore, the improved crystallinity of the intrinsic layer in the triple-GPL structure allows more photon absorption in a wider optical spectrum. Moreover, a better crystallinity of the intrinsic layer results in a smaller defect density at the interface between the p-layer and the intrinsic layer. The decrease in the defect density at the interface may reduce carrier recombination and the leakage current in the solar cell, and thus improves the J_{sc}. Besides, the low defect density due to the good crystallinity of the intrinsic layer can also improve the FF of the triple-GPL structured solar cells, which may be greatly deteriorated by carrier recombination and current leakage.[20]

The high J_{sc} of the triple-GPL structured solar cell may also be related to a high light-trapping efficiency of the cell due to the graded refractive index of the GPL multilayer. Figure 6 shows the normalized J_{sc} of the single- and triple-GPL strucutred solar cells as a function of the sample tilting angle relative to the light source. As the sample tilting angle larger than 30°, the triple-GPL structure exhibits a higher normalized J_{sc} than the single-GPL structure. The refractive index (n) measurement shows that the triple-GPL layer has three regions with the n value decreasing (3.7, 3.5 and 3.3) with increasing the hydrogen dilution ratio, D_H. A lower refractive index

Table I. The photovoltaic performance of μc-Si:H solar cells with different GPL structures.

Device	V_{oc}(mV)	J_{sc}(mA)	FF	η(%)
Single -GPL structure	340	7.66	30.4	0.79
Double-GPL structure	390	5.96	48.9	1.16
Triple-GPL structure	450	19.7	50.6	4.5

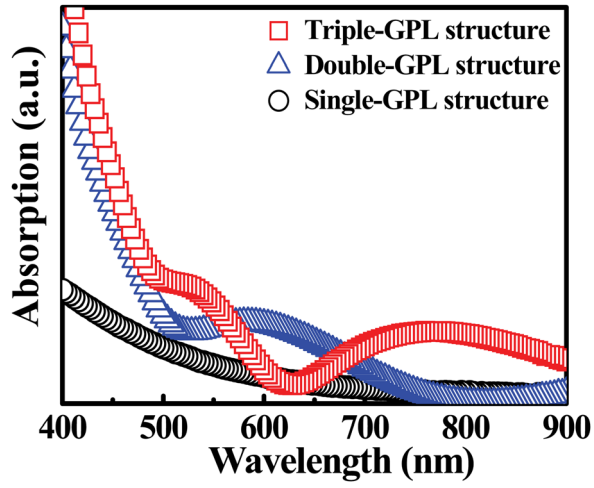

Figure 5. (Color online) The absorption spectrum of single-, double- and triple-GPL structured capping 50 nm intrinsic layers.

Downloaded on 2014-04-24 to IP 140.113.38.11 address. Redistribution subject to ECS terms of use (see ecsdl.org/site/terms_use) unless CC License in place (see abstract).

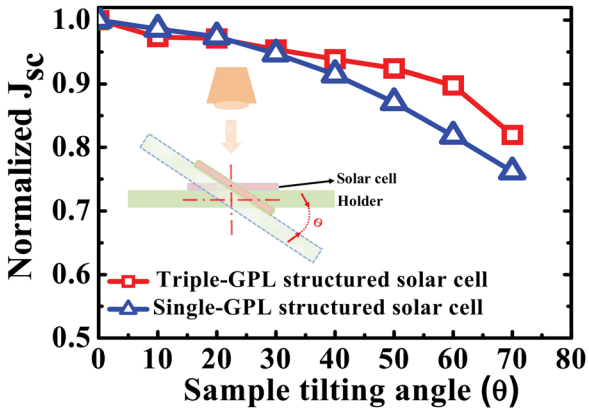

Figure 6. (Color online) The normalized J_{sc} as a function of sample tilting angle with the single-GPL and triple-GPL structured μc-Si:H solar cells from 0 to 70°. The geometric arrangement of the measurement with a fixed light source is also schematically illustrated.

indicates a lower film density, which can be achieved by improving the film crystallinity.[21] The graded refractive index of the triple-GPL layer may enhance antireflection in the solar cell, leading to greater photon absorption in the intrinsic layer and thus increasing the J_{sc}.

Conclusion

We have fabricated μc-Si:H thin film solar cells by HWCVD using hydrogen dilution profiling in the p-layer. The plasma-free HWCVD can produce the p-layer without the incubation amorphous layer, which is usually found in μc-Si:H thin films deposited by plasma-assisted CVD. The triple-GPL cell demonstrates better photovoltaic performance than the single- and double-GPL cells. The triple-GPL solar cell exhibits a conversion efficiency of 4.5%. The improvement in the photovoltaic performance is ascribed to that the triple-GPL cell has better crystallinity in the p-layer and the absorption layer as a result of the absence of plasma damage during the HWCVD process, which leads to the elimination of the incubation layer and better film crystallinity. Because of the good crystallinity and the multiple graded hydrogen concentration, the triple-GPL cell has a low defect density, high light absorption in the near IR regime and an improved antireflection efficiency. As a consequence, the triple-GPL structured μc-Si:H thin film solar cell has a great improvement in the fill factor, the conversion efficiency and the quantum efficiency.

Acknowledgments

The authors thank the National Science Council of the Republic of China for financial supports. The technical support form National Nano device Laboratories (NDL) is also gratefully acknowledged.

References

1. J. Meier, R. Flückiger, H. Keppner, and A. Shah, *Appl. Phys. Lett.*, **65**, 860 (1994).
2. A. Shah, P. Torres, R. Tscharner, N. Wyrsch, and H. Keppner, *Science*, **285**, 692 (1999).
3. S. R. Jadkar, J. V. Sali, M. G. Takwale, D. V. Musale, and S. T. Kshirsagar, *Thin Solid Films*, **395**, 206 (2001).
4. H. Li, R. H. Franken, R. L. Stolk, C. H. M. van der Werf, J. K. Rath, and R. E. I. Schropp, *J. Non-Cryst. Solids*., **354**, 2087 (2008).
5. P. Gogoi and P. Agarwal, *Sol. Energy Mater. Sol. Cells*., **93**, 199 (2009).
6. R. E. I. Schropp and M. Zeman, *Amorphous and Microcrystalline Silicon Solar Cells: Modeling, Materials and Device Technology*, p. 25, Academic Publishers, Norwell (1998).
7. O. Vetterl, F. Finger, R. Carius, P. Hapke, L. Houben, O. Kluth, A. Lambertz, A. Mück, B. Rech, and H. Wagner, *Sol. Energy Mater. Sol. Cells*, **62**, 97 (2009).
8. J. Li, J. Wang, M. Yin, P. Gao, Q. Chen, Y. Li, and D. He, *J. Cryst. Growth*, **310**, 4340 (2008).
9. B. Yan, G. Yue, J. Yang, S. Guha, D. L. Williamson, D. Han, and C. Jiang, *Appl. Phys. Lett.*, **85**, 1955 (2004).
10. J. Gu, M. Zhu, L. Wang, F. Liu, B. Zhou, and Y. Zhou, *J. Appl. Phys.*, **98**, 093505 (2005).
11. S. Liu, X. Zeng, W. Peng, H. Xiao, W. Yao, X. Xie, C. Wang, and Z. Wang, *J. Non-Cryst. Solids*, **357**, 121 (2011).
12. J. H. Zhou, K. Ikuta, T. Yasuda, T. Umeda, S. Yamasaki, and K. Tanaka, *Appl. Phys. Lett.*, **71**, 1534 (1997).
13. S. A. Filonovich, M. Ribeiro, A. G. Rolo, and P. Alpuim, *Thin Solid Films*, **516**, 576 (2008).
14. P. R.i Cabarrocas, A. F.i Morral, S. Lebib, and Y. Poissant, *Pure Appl. Chem.*, **74**, 359 (2002).
15. G. Viera, S. Huet, M. Mikikian, and L. Boufendi, *Thin Solid Films*, **403**, 467 (2002).
16. J. E. Bourée, *Thin Solid Films*, **395**, 157 (2001).
17. M. A. Green, *Solar Cells: Operating Principles, Technology and System Applications*, p. 86, N.S.W.: University of New South Wales, Kensington (1986).
18. H. Chen, M. H. Gullanara, and W. Z. Shena, *J. Cryst. Growth*, **91**, 260 (2004).
19. M. Yoon, K. Im, J.Yang, and S. Lim, *Physica B*, **405**, 1526 (2010).
20. M. Python, E. Vallat-Sauvain, J. Bailat, D. Dominé, L. Fesquet, A. Shah, and C. Ballif, *J. Non-Cryst. Solids*, **354**, 2258 (2008).
21. J. Müllerová, S. Jurečka, and P. Sutta, *Solar Energy*, **80**, 667 (2006).

Downloaded on 2014-04-24 to IP 140.113.38.11 address. Redistribution subject to ECS terms of use (see ecsdl.org/site/terms_use) unless CC License in place (see abstract).